Structure of the Intrinsic Shallow Electron Center in AgCl Studied by Pulsed Electron Nuclear Double Resonance Spectroscopy at 95 GHz

M. T. Bennebroek,[1] O. G. Poluektov,[1] A. J. Zakrzewski,[2] P. G. Baranov,[3] and J. Schmidt[1]

[1]*Centre for the Study of the Excited States of Molecules, Leiden University, P.O. Box 9504, NL-2300 RA Leiden, The Netherlands*

[2]*Institute of Physics, Polish Academy of Sciences, Al. Lotnikow 32/46, 02-668 Warsaw, Poland*

[3]*A.F. Ioffe Physico-Technical Institute, Polyteknicheskaya 26, 194021 St. Petersburg, Russia*

(Received 31 August 1994)

In this Letter we report the first direct determination of the wave function of the intrinsic shallow electron center in silver chloride. A model is suggested in which an electron is shallowly trapped by two adjacent silver ions on a single cationic site. The information has been obtained by pulsed electron nuclear double resonance at 95 GHz and illustrates the potential of high-frequency EPR techniques for the study of defects in semiconductors.

PACS numbers: 71.50.+t, 61.72.Ji, 76.70.Dx, 82.50.Fv

Intrinsic defect centers in inorganic crystals have attracted considerable attention, because of their importance for material science. In particular, the F center in alkali halides has occupied a central place. The identification of its structure was eventually solved by electron nuclear double resonance (ENDOR) spectroscopy. The results proved that this center consists of an electron trapped in the Coulombic field of a (substitutional) anion vacancy and that the alternative model, which assumed the presence of an electron bound to an interstitial cation, had to be rejected [1].

The identification of the structure of the intrinsic shallow electron center in silver halides resembles the problem concerning the F center. Shallow electron centers are created upon uv excitation and are believed to play an important role in the latent image formation process [2,3]. They can be studied at low temperatures and were first observed in 1969 by Brandt and Brown using uv-induced infrared absorption spectroscopy [4]. It was suggested that the intrinsic binding core consists of an interstitial silver ion [5], but other models include a substitutional silver ion at a surface kink or an internal jog [2]. The intrinsic shallow electron centers have also been observed by EPR spectroscopy and they give an isotropic, structureless line at $g \sim 1.88$ in AgCl [6] and $g \sim 1.49$ in AgBr [7]. Until now, both optical and EPR spectroscopy have been unable to establish the structure of the binding core.

In this Letter we report the first ENDOR spectra of intrinsic shallow electron centers in AgCl. They allow us to determine the spatial delocalization of the loosely bound electron and to propose a model for the binding core. The conclusions are supported by similar ENDOR results on the self-trapped exciton (STE) and on electrons shallowly bound to divalent cationic impurities.

The ENDOR spectra were obtained via a method which is based on the stimulated echo (SE) pulse sequence [8]. Here a $\pi/2$-τ-$\pi/2$-T-$\pi/2$ microwave pulse sequence is applied resonant with the EPR signal of the shallow electron center at $g = 1.878$. The SE signal is produced at time τ after the third $\pi/2$ pulse. A radio frequency (RF) pulse between the second and third $\pi/2$ pulse induces the nuclear transitions and its effect is monitored as a decrease of the SE intensity. The ENDOR spectra were recorded at 1.2 K with a spectrometer operating at a microwave frequency of 95 GHz. The spectrometer and its specific advantages for this work will be described in detail elsewhere [9]. The main experiment has been performed on an undoped AgCl crystal of which the EPR spectrum has been published previously [10].

In Figs. 1(a) and 1(b) the ENDOR spectrum of the shallow electron center is presented. The ENDOR transitions of silver nuclei are shown in Fig. 1(a) where the nuclear Zeeman frequencies of ^{107}Ag ($I = 1/2$, 52%) and ^{109}Ag ($I = 1/2$, 48%) are observable as dips at 6.224 and 7.156 MHz, respectively. Figure 1(b) shows the chlorine ENDOR transitions and the dips at 12.537 and 15.057 MHz indicate the nuclear Zeeman frequencies of ^{35}Cl ($I = 3/2$, 76%) and ^{37}Cl ($I = 3/2$, 24%), respectively. The ENDOR spectra proved to be isotropic apart from a few lines in the chlorine spectrum which exhibit a quadrupole splitting.

The ENDOR spectra of Figs. 1(a) and 1(b) can be analyzed using the Hamiltonian

$$\mathcal{H} = g_e\beta_e\mathbf{B}_0 \cdot \mathbf{S} - \sum_\alpha (g_{n\alpha}\beta_n\mathbf{B}_0 \cdot \mathbf{I} + \mathbf{a}_\alpha\mathbf{S} \cdot \mathbf{I}_{\alpha\alpha} + \mathbf{I}_\alpha \cdot \mathbf{Q}_\alpha \cdot \mathbf{I}_\alpha), \quad (1)$$

which describes an electron spin, with operator $\mathbf{S}$, coupled to a collection of nuclear spins, with operators $\mathbf{I}_\alpha$, in a static magnetic field $\mathbf{B}_0$. Here the first two terms on the right describe the electron and nuclear Zeeman interaction with g_e the electron and $g_{n\alpha}$ the nuclear g factors. β_e is the Bohr and β_n the nuclear magneton. The third term describes the isotropic superhyperfine interaction with the hyperfine constant a_α given by

$$a_\alpha = \frac{8\pi}{3} g_e\beta_e g_{n\alpha}\beta_n |\Psi(\alpha)|^2. \quad (2)$$

Here $|\Psi(\alpha)|^2$ reflects the spin density on nucleus α. The traceless tensor $\mathbf{Q}_\alpha$ reflects the quadrupole interaction of

 0031-9007/95/74(3)/442(4)$06.00

the chlorine nuclei ($I = 3/2$). The intensity of the few ENDOR lines which exhibit a quadrupole splitting was so weak that we were unable to resolve their orientational dependence and therefore we will not discuss them here. In case of an electron spin ($S = 1/2$) coupled to a single silver nucleus ($I = 1/2$) and using first order perturbation theory, one can derive from expression (1) that the ENDOR transitions, corresponding to $\Delta M_S = 0$ and $\Delta M_I = \pm 1$, have the following frequencies:

$$\nu_{\mathrm{ENDOR}}(\alpha) = \frac{1}{h}\left| g_{n\alpha}\beta_n B_0 \pm \frac{a_\alpha}{2} \right| . \qquad (3)$$

For a chlorine nucleus ($I = 3/2$) the same expression holds when the quadrupole interaction is neglected. Therefore expression (3) predicts that each nucleus α will give rise to two ENDOR transitions symmetrically placed around their nuclear Zeeman frequency $g_{n\alpha}\beta_n B_0/h$. This behavior is indeed observed in the recorded spectra of Figs. 1(a) and 1(b). The fact that a multitude of lines is present indicates that we are dealing with a delocalized electron which interacts with a large number of Ag and Cl nuclei.

For a quantitative analysis of the observed superhyperfine constants, expression (2) indicates that it is necessary to determine the spin density $|\Psi(\alpha)|^2$ on each nucleus α. This problem has already been studied for the case of color centers in alkali halides, particularly the F center. Gourary and Adrian [11] showed that, by orthogonalizing a suitable envelope function Φ to the cores of the lattice ions in order to allow for the Pauli principle, the spin density on nucleus α may be written as an "amplification factor" A_α times the density of the envelope function Φ on that nucleus. Thus $|\Psi(\alpha)|^2 = A_\alpha|\Phi(\alpha)|^2$. If the envelope function remains approximately constant within each ion core, the value of A_α will only depend on the species of ion α and not on its position in the lattice. We then rewrite equation (2) to

$$a_\alpha = \frac{8\pi}{3} g_e\beta_e g_{n\alpha}\beta_n A_\alpha |\Phi(\alpha)|^2. \qquad (4)$$

Our analysis is based on the prediction of effective mass theory (EMT) that the ground state of shallow donors in semiconductors can be described by a hydrogenlike $1s$ wave function $\Phi(r) \sim \exp(-r/r_0)$ [12]. We used a trial-and-error procedure in which we calculated $|\Phi(\alpha)|^2$ on a large number of Ag and Cl positions in the cubic AgCl lattice, trying various center positions of Φ and by optimizing the values of A_{Ag}, A_{Cl} and the Bohr radius r_0 to match the observed hyperfine constants.

The result of our analysis is shown in Fig. 2 where the density of Φ is plotted as a function of r. This result is based on the assumption that Φ is centered on a Ag^+ lattice position. It is convenient to define shells consisting of nuclei with the same radius r. We have been able to derive the density of the envelope function on a large number of Ag and Cl shells and some of the Ag shells are indicated in Fig. 2. It turned out that for shells with a radius larger than ~12 Å the derived electron densities indeed obey the expected exponential form with a Bohr radius $r_0 = 17.2 \pm 0.6$ Å; however, for nearby shells there is a clear deviation. We think that this results from the neglect of the influence of the chemical nature of the binding center and it illustrates the need of the so-called central cell correction in EMT [12]. Part of this deviation may also result from a breakdown of our assumption that A_α does not depend on the lattice position of nucleus α.

The derived densities can be very well described by the following normalized monotonically decreasing function:

$$|\Phi(r)|^2 = \frac{1}{7\pi r_1}(1 + r/r_1)^2 e^{-2r/r_1}. \qquad (5)$$

Possible deviations with respect to this monotonical decrease have not been taken into account. For comparison we plotted function (5) in Fig. 2 using $r_1 = 9.94$ Å, $A_{\mathrm{Ag}} = 2450$, and $A_{\mathrm{Cl}} = 1060$.

The experimental ENDOR spectrum was simulated by calculating the frequency of an ENDOR transition using Eqs. (4) and (5) and by taking the number of nuclei in a shell as a relative measure for the ENDOR intensity. The

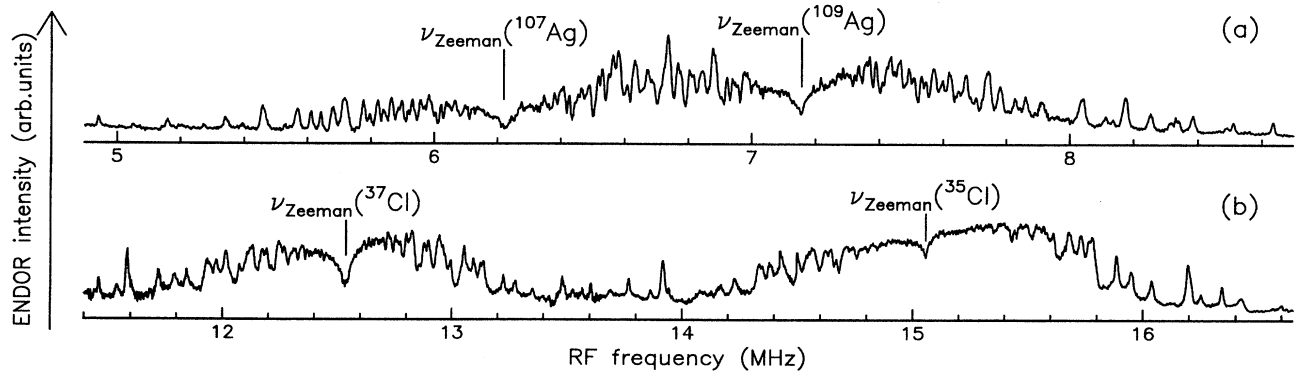

FIG. 1. The silver (a) and chlorine (b) ENDOR spectra of the $g = 1.878$ shallow electron center ($S = 1/2$). Typical pulse lengths: $\pi/2 = 100$ ns, τ between 400 and 900 ns, $T = 700$ μs and the length of the RF pulse = 600 μs.

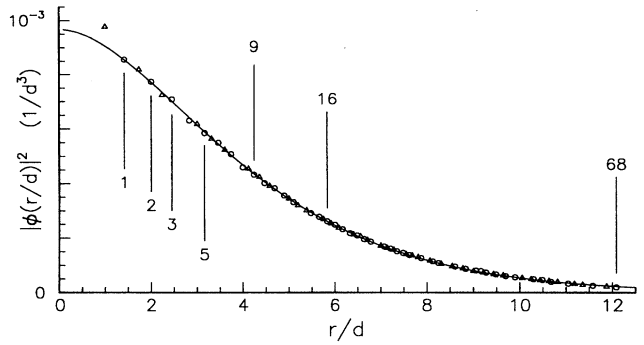

FIG. 2. The density of the envelope function of the shallow electron center as a function of r/d with the interionic distance $d = 2.7532$ Å at 0 K. The open circles and triangles denote the densities derived from the Ag and Cl ENDOR spectra, respectively. Some neighboring silver shells are indicated. The solid line reflects function (5).

result of such a simulation of the high-frequency part of the ^{109}Ag ENDOR spectrum is shown in Fig. 3(a), where it is compared to the recorded spectrum. The figure shows a good overall agreement between the recorded and the simulated spectrum. The simulation, however, does not account for all features observed at frequencies above 8.1 MHz. The ENDOR lines in this region correspond to shells that lie close to the center of Φ and suggest the presence of a lattice distortion in the direct surrounding of the binding core. We indicated the ENDOR transitions of some of the Ag shells together with the corresponding number of nuclei in each shell and it is seen that even the contribution of the 68th silver shell can be resolved. Figure 3(b) compares the recorded spectrum of the low-frequency part of the ^{37}Cl ENDOR to its corresponding simulation. Again a good overall agreement is obtained and the contributions up to the 49th chlorine shell can be observed.

The results depicted in Figs. 2 and 3 were obtained by placing the center of the envelope function Φ on a Ag^+ lattice position and this turned out to be the only position for which we could obtain a satisfactory analysis of our Ag and Cl ENDOR spectra. A displacement by only 4% of the interatomic distance in any direction would already spoil the agreement between the simulated and the recorded spectra.

We suggest that the shallow electron center is of intrinsic nature and not related to impurities. This is based on a comparison of our results with those obtained from uv-induced infrared absorption spectroscopy by Sakuragi and Kanzaki [5]. They measured the energy difference $E_{1s\text{-}2p}$ between the hydrogenlike $1s$ and $2p$ states of intrinsic and impurity-related shallow electron centers. Since the ENDOR results confirm that the shallow electron behaves very much like a hydrogenlike $1s$ electron with Bohr radius r_0, we can make an estimate of $E_{1s\text{-}2p}$ by using the hydrogen model [3]. Table I shows

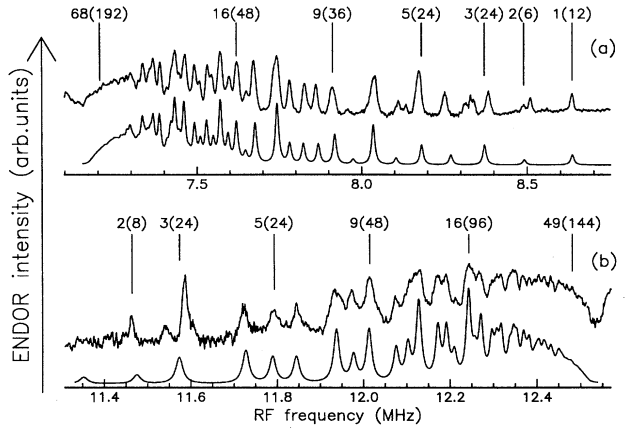

FIG. 3. (a) Comparison between the recorded (upper curve) and simulated (lower curve) high-frequency part of the ^{109}Ag ENDOR spectrum of the shallow electron center. (b) A similar comparison for the low-frequency part of the ^{37}Cl ENDOR spectrum. The first Cl shell is not observed in the ^{37}Cl ENDOR spectrum but is present in the ^{35}Cl spectrum. We used Lorentzians to represent ENDOR line shapes and the calculated spectrum is multiplied nearby the nuclear Zeeman frequency with the factor $1 - \cos[2\pi(\nu_{\mathrm{ENDOR}} - \nu_{\mathrm{Zeeman}})2\tau]$ to account for the frequency dependence of the ENDOR effect [17].

that the estimated energy in our undoped AgCl crystal is in agreement with the observed energy of intrinsic shallow electron centers.

Additional experiments on impurity-related shallow electron centers in Cd^{2+}- and Pb^{2+}-doped AgCl crystals, which also appear at $g = 1.878$ [13], yielded similar ENDOR spectra. The Bohr radii for these centers are also presented in Table I and it is seen that a good agreement exists between the estimated and observed values of $E_{1s\text{-}2p}$. This shows that the simple hydrogen model can successfully be applied for the calculation of this energy difference. Apparently the deviation of about 5% of the density of the electronic wave function from the $1s$-like behavior has only a negligible effect.

Information concerning the charge of the intrinsic shallow electron center can be obtained from ENDOR on the STE. The STE is created during uv excitation and in EPR the lowest excited $S = 1$, spin triplet state can be observed [10]. It consists of an electron loosely bound to a self-trapped hole (STH) and can therefore be considered

TABLE I. Column 2: the Bohr radius r_0 of the shallow electron centers in undoped, Pb^{2+}- and Cd^{2+}-doped AgCl, as obtained from the ENDOR data. Columns 3 and 4 show the estimated and experimentally observed energies $E_{1s\text{-}2p}$ [5], respectively.

Crystal	r_0 (Å)	$E^{\mathrm{calc}}_{1s\text{-}1p}$ (meV)	$E^{\mathrm{expt}}_{1s\text{-}1p}$ (meV)
AgCl: Cd^{2+}	15.7 ± 0.6	36.0 ± 1.4	34.9
AgCl: undoped	17.2 ± 0.6	32.9 ± 1.1	33.5
AgCl: Pb^{2+}	19.5 ± 0.9	29.0 ± 1.5	30.5

as a special case of a shallow electron center. In a forthcoming publication we will show that it is possible to derive the spatial distribution of the electronic part of the STE, in a similar way as described here for the intrinsic shallow electron center. We found that the shallowly trapped electron of the STE also behaves very much like a hydrogen $1s$ electron, centered on a Ag^+ lattice position, with a Bohr radius $r_0 = 16.4 \pm 0.9$ Å. The close agreement of this value with the one derived for the intrinsic shallow electron center ($r_0 = 17.2 \pm 0.6$ Å) and the fact that the electron of the STE is shallowly bound by the Coulombic field of a STH, indicates that the shallow electron center has the same Coulombic charge.

Since our results show that the intrinsic shallow electron center is located on a Ag^+ lattice position, we can reject the previously suggested model of an interstitial Ag^0 "atom" which consists of an electron loosely bound to a single interstitial Ag^+ ion. So far the ENDOR spectra give no direct information about the atomic structure of the core. To explain our observations we suggest that an interstitial Ag^0 atom is not stable but creates a molecular Ag_2^+ ion in which the unpaired electron is loosely bound to two adjacent Ag^+ ions, symmetrically placed around a Ag^+ lattice position. Such molecular Ag_2^{2+} ions have been observed in KCl crystals doped with silver after x irradiation at room temperature, however, in KCl they form, in contrast to the present situation, deep electron traps [14].

The unstable interstitial Ag^0 atom can be formed via the capture of an electron by an interstitial Ag^+ ion which is either "frozen-in" or created via Frenkel pair formation in the silver sublattice. In the latter case, the resulting Ag_2^+ ionic shallow electron center is formed simultaneously with a silver ion vacancy that is probably located nearby a charge-compensating STH. In alkali halides, the formation of Frenkel pairs during uv irradiation at low temperatures has been observed but, in contrast to silver halides, this process takes place in the halogen sublattice. For instance the pair in KCl consists of a molecular Cl_2 ionic hole center at an anionic lattice position (the H center) and an electron trapped at an anion vacancy (the F center) [15]. This pair can be looked upon as the antipode of the suggested pair in AgCl. It is known that Frenkel pairs in alkali halides are created by the nonradiative decay of STE's [15]. The same mechanism could be active in AgCl but calculations are necessary to check whether this process has sufficient efficiency. We note that circumstantial experimental evidence exists which suggests the formation of Frenkel pairs in silver halides at liquid helium temperatures [16].

In conclusion, the presented ENDOR results prove that the $g = 1.878$ paramagnetic center in undoped AgCl originates from a shallow electron center. Our analysis shows that the center is located on a Ag^+ lattice position within 4% of the interatomic distance and, based on a comparison of our results with optical data reported by Sakuragi and Kanzaki, we conclude that the center is of intrinsic origin. We suggest that the electron is shallowly trapped in the Coulombic field of two adjacent Ag^+ ions, symmetrically placed on a single cationic site. Such molecular Ag_2^+ ions can be formed either via frozen-in interstitial silver ions or via the formation of Frenkel defect pairs in a similar, but antimorphic, way as in alkali halides.

This work forms part of the research program of the Stichting voor Fundamenteel Onderzoek der Materie (FOM) with financial support from the Nederlandse Organisatie voor Wetenschappelijk Onderzoek (NWO). The authors wish to thank Dr. R. S. Eachus for very stimulating discussions.

[1] S. Seidel and H. C. Wolf, in *Physics of Color Centers,* edited by W. B. Fowler (Academic Press, New York and London, 1968).
[2] J. F. Hamilton, in *The Theory of the Photographic Process,* edited by T. H. James (The Macmillan Company, New York, 1977).
[3] A. P. Marchetti and R. S. Eachus, Adv. Photochem. **17**, 145 (1992).
[4] R. C. Brandt and F. C. Brown, Phys. Rev. **181**, 1241 (1969).
[5] S. Sakuragi and H. Kanzaki, Phys. Rev. Lett. **38**, 1302 (1977).
[6] R. S. Eachus, R. E. Graves, and M. T. Olm, Phys. Status Solidi (b) **152**, 583 (1989).
[7] J. Z. Brescia, R. S. Eachus, R. Janes, and M. T. Olm, Cryst. Latt. Def. Amorph. Mat. **17**, 165 (1987).
[8] W. B. Mims, in *Electron Paramagnetic Resonance,* edited by S. Geschwindt (Plenum, New York, 1972).
[9] J. A. J. M. Disselhorst, H. J. van der Meer, O. G. Poluektov, and J. Schmidt (to be published).
[10] O. G. Poluektov, M. C. J. M. Donckers, P. G. Baranov, and J. Schmidt, Phys. Rev. B **47**, 10 226 (1993).
[11] B. S. Gourary and F. J. Adrian, Phys. Rev. **105**, 1180 (1957).
[12] K. W. Böer, *Survey of Semiconductor Physics* (Van Nostrand Reinhold, New York, 1990).
[13] R. S. Eachus, R. E. Graves, and M. T. Olm, Phys. Status Solidi (b) **88**, 705 (1978).
[14] R. A. Zhitnikov, P. G. Baranov, and N. I. Melnikov, Phys. Status Solidi (b) **59**, k111 (1973).
[15] W. Hayes and A. M. Stoneham, *Defects and Defect Processes in Nonmetallic Solids* (John Wiley & Sons, Inc., New York, 1985).
[16] H. Kanzaki, Semicond. Insul. **5**, 517 (1983).
[17] C. Gemperle and A. Schweiger, Chem. Rev. **91**, 1481 (1991).